EPJ Web of Conferences **193**, 01005 (2018) https://doi.org/10.1051/epjconf/201819301005
FISSION 2017

First signs of collectivity in $N = 86$ and 88 isotones above ^{132}Sn

Houda NAÏDJA[1,2,⋆] and *Frédéric* NOWACKI[1,⋆⋆]

[1] *Université de Strasbourg, CNRS, IPHC UMR 7178, F-67000 Strasbourg, France*
[2] *Université Constantine 1, LPMPS, route Ain El Bey 25000 Constantine, Algeria*

Abstract. Within the shell-model framework the low-lying states energies, E2 and M1 transitions of chains of nuclei $52 \leq Z \leq 60$ with $82 \leq N \leq 88$ are investigated. We use the N3LOP effective interaction derived from Effective Field Theory Potentials and phenomenologically constrained. We noticed clear collective features in $N = 86$ and 88 isotones, with signature of triaxial $\gamma-$bands.

1 Introduction

Investigation of neutron rich nuclei in the vicinity of the robust ^{132}Sn core represents currently an attractive subject of nuclear structure research. Recent advances in radioactive-ion-beam facilities and detection systems provided access to many exotic nuclei in this region. At the same time the continuous progress in the development of computational codes to treat the shell-model numerical challenge allied with development of modern realistic effective interactions opens new opportunities of successful theoretical approaches, to explore and gain more information from this heavy mass region nuclei.

In this context, the low-lying spectra, E2 and M1 transition strengths of even-even chains of nuclei with $52 \leq Z \leq 60$ and $82 \leq N \leq 88$ are explored and extended compared to our previous works [1–3]. Special attention is devoted to the collectivity in the $N = 86$ and 88 isotones, where the investigation of their quadrupole properties and the shape degrees of freedom (β, γ) exhibits the occurrence of soft triaxial γ-bands.

The paper is organized as follows: After a briefly review in section 2 of shell-model tools used in this part of work, we expose in section 3 the energy levels, and the electromagnetic transitions of the nuclei of interest. The features of collectivity in $N = 86$ and 88 isotones are widely discussed in section 4, with gathering the conclusions in section 5.

2 shell-model pieces

2.1 Valence space

The shell-model calculations are performed in the model space $r4h - r5i$ (using the same notation in [4]), including $1f_{7/2}, 0h_{9/2}, 1f_{5/2}, 2p_{3/2}, 2p_{1/2}, 0i_{13/2}$ orbitals for neutrons and

⋆ e-mail: nhouda@gmail.com
⋆⋆ e-mail: frederic.nowacki@iphc.cnrs.fr

© The Authors, published by EDP Sciences. This is an open access article distributed under the terms of the Creative Commons Attribution License 4.0 (http://creativecommons.org/licenses/by/4.0/).

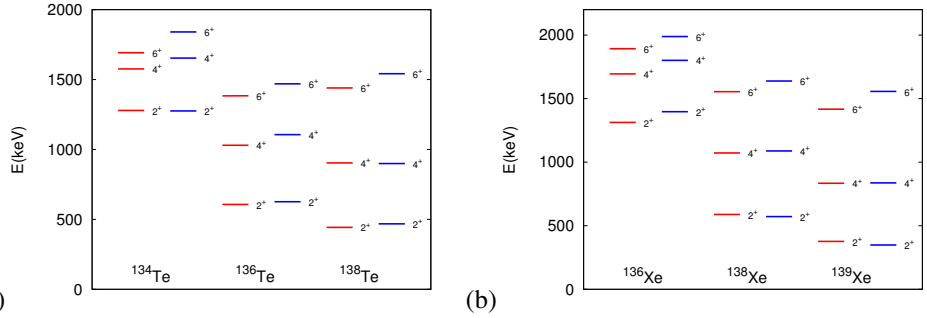

Figure 1. Low-lying state energies of (a) ^{134,136,138}Te and (b) ^{136,138,140}Xe calculated using N3LOP interaction (blue line) compared to the data (red line).

$0g_{7/2}, 1d_{5/2}, 1d_{3/2}, 2s_{1/2}, 0h_{11/2}$ orbitals for protons, taken above a closed ^{132}Sn core. The corresponding neutrons and protons single particle energies are fixed from ^{133}Sn and ^{133}Sb experimental data [5] respectively. However the $0i_{13/2}$ neutron and $2s_{1/2}$ proton orbital energies are taken as empirical values from [6] and [7] respectively.

With such a valence space the diagonalization using ANTOINE and NATHAN shell-model codes [8, 9] is a real challenge, and we face up to huge dimensions of Hamiltonian matrices (example 2.10^{11} in m-scheme in the case of ^{146}Nd).

2.2 Effective interaction

As a starting point we derived a realistic interaction V_{NN} from Chiral effective field theory potentials N3LO [10]. Handling with such potentials having a strong repulsive core was overcome by making use to the so called low momentum approach V_{low-k}, obtained by integrating V_{NN} down to a cutoff momentum $\wedge$=$2.2fm^{-1}$. This renormalized interaction will be adapted to the model space by many body perturbation theory techniques, including all the $\hat{Q}$-box folded-diagrams up to the second order [11].

Reducing the $1f_{7/2}$ neutron-neutron pairing matrix element of N3LO realistic interaction (by about 120 keV) was necessary, to obtain the observed isomeric transition in the mid-shell nucleus ^{136}Sn, where the initial realistic interaction failed to reproduce it. The quenching of these transitions rates at mid-shell is due to a seniority mixing effect as discussed extensively in our earlier following works [1, 2, 12]. The resulting interaction named hereafter by N3LOP was applied to inspect the spectroscopic properties and the collectivity of chains of $82 \leq N \leq 88$ isotones.

3 Low-lying state energies, E2 and M1 transitions

The low-lying state energies of chains of nuclei Te, Xe, Ba, Ce and Nd with $82 \leq N \leq 86$ gathered in figures 1, 2, 3 are very well reproduced compared to the data [5]. The compression of some excited states energies in ^{144}Ce and ^{146}Nd is justified by an effect of the truncations adopted in these cases, where we kept up to 4p-4h excitations. One should stress that the appropriate truncations ensure the good convergence of energy levels and preserve the collective properties. Also we note a decrease of 2^+ energies by increasing the neutron number, reflecting the presence of collectivity in these systems (see sect.4).

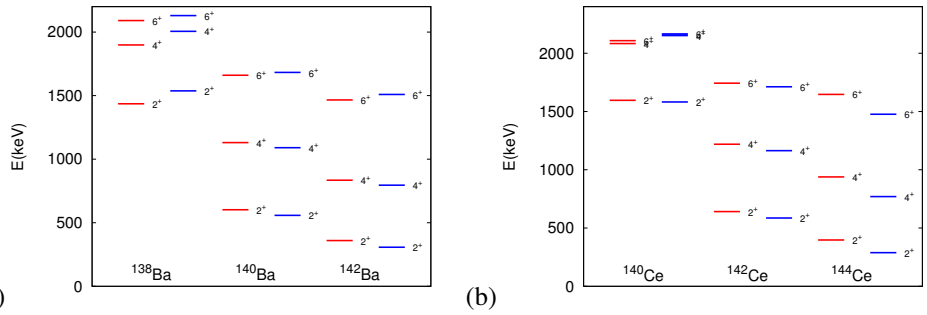

Figure 2. Low-lying state energies of(a) ^{138,140,142}Ba and (b) ^{140,142,144}Ce calculated using N3LOP interaction (blue line) compared to the data (red line).

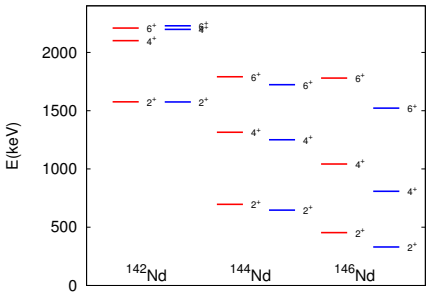

Figure 3. Low-lying state energies of ^{142,144,146}Nd calculated using N3LOP interaction (blue line) compared to the data (red line).

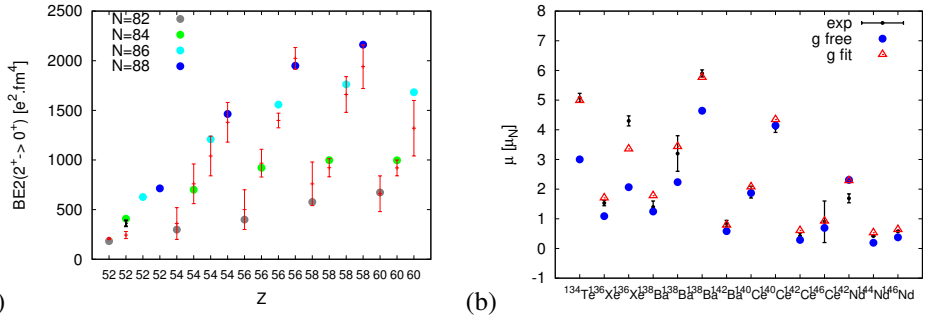

Figure 4. (a) The calculated $B(E2, 2^+ \rightarrow 0^+)$ transitions of different isotones (circles) and (b) their magnetic moments μ of $2^+, 4^+$ and 6^+ states, compared to the data.

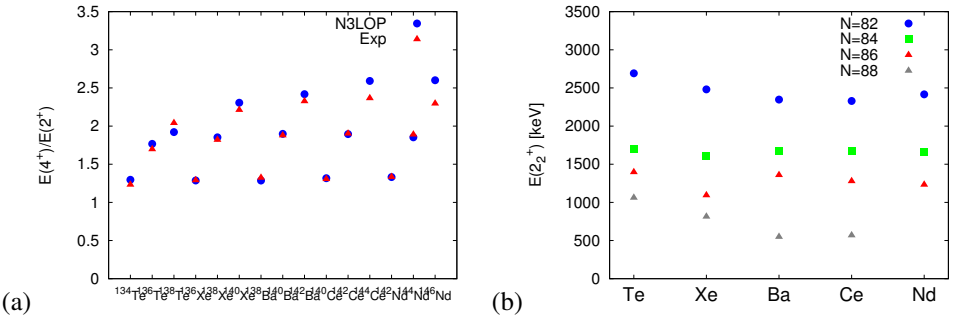

Figure 5. (a) Variation of the energy ratio $E(4^+)/E(2^+)$, and (b) the 2_2^+ energies in different isotones.

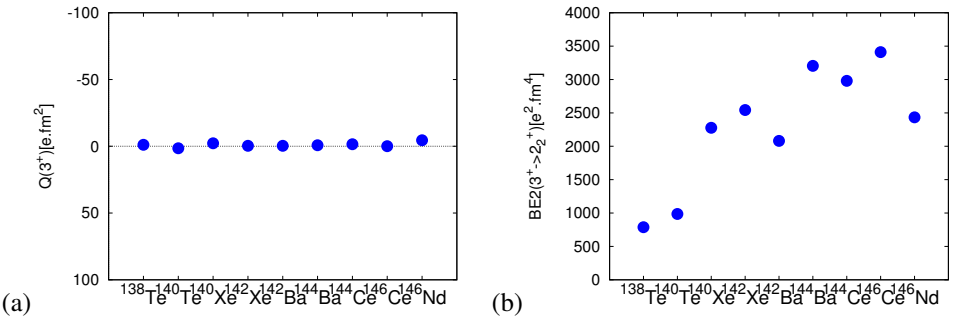

Figure 6. (a) Variation of 3^+ quadrupole moment, and (b) the transitions $B(E2, 3^+ \rightarrow 2_2^+)$.

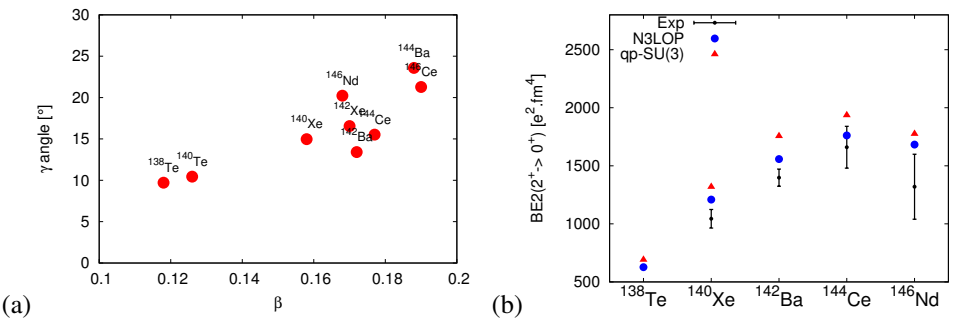

Figure 7. (a) The shape parameters of $N = 86$ and 88 isotones, and (b) the effect of the combination between pseudo and quasi SU(3) symmetries to the quadrupole transitions.

The $B(E2, 2^+ \rightarrow 0^+)$ electric transitions of different $N = 82, 84, 86$, and 88 isotones reported in figure 4a indicate an excellent agreement with the data [5] using effective charges $0.6e$ for neutrons and $1.6e$ for protons. It is important to notice the calculated value in ^{136}Te overestimated when compared to the previous unexpected data [13] (red error bar), is now consistent with the new measurement of [14] (black error bar). Also we can observe a marked increase of the transitions with increasing neutron number, reflecting a transition from spherical character in the $N = 82$ isotones to collective character in $N = 86$ and 88 isotones.

The magnetic moments of $2^+, 4^+$ and 6^+ states for different nuclei in this mass region displayed in figure 4b, and compared to the data [15] are calculated using two sets of spin and orbital g factors. Employing the free g-factors $(g_\pi^s, g_\pi^l) = (5.5857, 1.0)$ for protons and $(g_\nu^s, g_\nu^l) = (-3.8263, 0.0)$ for neutrons, the agreement is quite poor due to the renormalization of the effective operators induced by the missing of some spin orbit partners in our model space. However, the second set of calculations achieved using the effective g-factors $(g_\pi^s, g_\pi^l) = (3.250, 1.069)$ for protons and $(g_\nu^s, g_\nu^l) = (-1.506, 0.019)$ for neutrons improve greatly the accord with the data. The new values are obtained by adjustment to reproduce the available data [15] for the magnetic moments of $N = 82, 84, 86$ isotones.

4 Collectivity in $N = 86$ and 88 isotones

Particular attention is devoted to $N = 86$ and 88 isotones marked by very strong strength transitions (figure 4a), the energy ratio $E(4^+)/E(2^+) \sim 2.4$ is typical to transitional nuclei (figure 5a), with very low-lying 2_2^+ energies (figure 5b), indicating the presence of large quadrupole correlations. Besides, the investigation of quadrupole spectroscopic properties of these systems unveils striking features, such as :

- $Q_s(2_\gamma^+, K = 2)$ is nearly equal with an opposite sign to $Q_s(2^+, K = 0)$
- $Q_s(3^+, K = 2)$ is close to zero and the low-lying 3^+ state is connected by a strong transition to the 2_γ^+ state.

All these aspects displayed in figures 6a and 6b, fulfilled the criteria of deformed nuclei, characterized by triaxial $\gamma-$band, where the 2_2^+ is a head of these $K = 2$ γ-bands.

To strengthen our predictions about the triaxiality in these systems, we have calculated β deformation parameter and γ angle from Kumar's geometric model [16]. These parameters give us more relevant information about the intrinsic shapes. From the set of β and γ values ascribed to the chains of $N = 86$ and 88 isotones (figure 7a), we can ascribe mild deformation in Te isotopes and a visible increase of deformation with non-axiality from ^{140}Xe to ^{146}Nd, reaching the maximum in ^{146}Ce. This enhancement of the collectivity can be easily understood by Elliott's SU(3) algebraic model [17].

In this context, we have compared in figure 7b, the $BE2(2^+ \rightarrow 0^+)$ transitions of $N = 86$ isotonic chain, calculated within different cases of algebraic SU(3) framework:

- In pseudo-SU(3) scheme, the orbits have the same angular momentum j sequences as those of full major oscillator shell, except the largest one ($g_{9/2}$), which is the case of $g_{7/2}, d_{5/2}, d_{3/2}, s_{1/2}$ proton orbits sequence in our model space.
- In quasi-SU(3) scheme the orbits are identified by $\Delta j = 2, \Delta l = 2$, which is the case of $f_{7/2} - p_{3/2}$ neutron orbits sequence in our model space.

In figure 7b, we show the full space calculations compared to the ones restricted to the combination between pseudo and quasi-SU(3) valence spaces for protons and neutrons respectively. These restrictions have a minor impact on the quadrupole transitions and confirms the validity of these approximations. However, including the proton excitations to $h_{11/2}$ orbit in N3LOP full calculations

reduces slightly the transitions. This could be understood as a pairing effect, as already observed in our previous conclusion in the study of ^{140}Sm low-lying states energies [18].

5 Conclusions

In conclusion, using the same effective interaction N3LOP, the spectroscopic properties of chains of nuclei Te, Xe, Ba, Ce and Nd with $82 \leq N \leq 88$ are investigated, where a convincing agreement appears between our results and the experimental data.

Additionally, the first clues of collectivity in $N = 86$ and 88 isotones was discussed, where the signs of soft $\gamma-$band are supported by the quadrupole properties and the deformation parameters. The evolution of this collectivity is sensitive to SU(3) symmetries of neutrons and protons orbit sequences.

Finally, we stress that the present results constitute a stringent test of N3LOP effective interaction and a benchmark for future experimental measurements. In this context our results are combined to the experimental data in the analysis of the high-spin states and the collectivity in ^{142}Ba and ^{144}Ce nuclei [19].

References

[1] H. Naïdja, F. Nowacki, and K. Sieja, J. Phys. Conf. Series **580**, 012030 (2015).
[2] H. Naïdja, F. Nowacki, and K. Sieja, Acta. Phys. Pol. B **46**, 669 (2015).
[3] H. Naïdja and F. Nowacki Acta. Phys. Pol. B **48**, 587 (2017).
[4] A. P. Zuker, Phys. Rev. Lett. **90** 042502 (2003).
[5] NNDC National Nuclear Data Center, Brookhaven National Laboratory, http://www.nndc.bnl.gov
[6] W. Urban, W. Kurcewicz, A. Nowak, T. Rzaca-Urban *et al.*, Eur. Phys. J **5**, 239 (1999).
[7] F. Andreozzi, L. Coraggio, A. Covello, A. Gargano, T. T. S. Kuo and A. Porrino, Phys. Rev. C **56**, R16 (1997).
[8] E. Caurier, G. Martinez-Pinedo, F. Nowacki, A. Poves and A.P. Zuker, Rev. Mod. Phys. **77**, 427 (2005).
[9] E. Caurier and F. Nowacki, Acta. Phys. Pol. B**30**, 705 (1999).
[10] D. Entem and R. Machleidt, Phys. Rev C. **68**, 0411001 (2003).
[11] M. Hjorth-Jensen, T.T.S. Kuo, and E. Osnes, Rev. Rep **261**, 125 (1995).
[12] G. S. Simpson, G. Gey, A. Jungclaus, J. Taprogge, S. Nishimura, *et al.*, Phys. Rev. Lett **113**, 132502 (2014).
[13] J. Shergur, B. A. Brown, V. Fedoseyev, U. Köster, K.-L. Kratz, D. Seweryniak, W. B. Walters, *et al*, Phys. Rev. C **65**, 034313(2002).
[14] J. M. Allmond, A. E. Stuchbery, C. Baktash, A. Gargano *et al.*. Phys. Rev. Lett **118**, 092503 (2017).
[15] N. J. Stone, Atomic Data and Nuclear Data Tables **90**, 75 (2005).
[16] K. Kumar, Phys. Rev. Lett. **28**, 249 (1972).
[17] J. P. Elliott, Proc. R. Soc. London **245**, 128 (1958).
[18] M. Klintefjord, K. Hadyńska-Klęk, A. Görgen, *et al*, Phys. Rev. C **93**, 054303 (2016).
[19] H. Naïdja, F. Nowacki *et .al* Phys. Rev. C **95**, 064303 (2017).